Environmental Research 183 (2020) 109149

Contents lists available at ScienceDirect

Environmental Research

journal homepage: www.elsevier.com/locate/envres

Mapping groundwater resiliency under climate change scenarios: A case study of Kathmandu Valley, Nepal

Sangam Shrestha[a,*], Sanjiv Neupane[a], S Mohanasundaram[a], Vishnu P. Pandey[b]

[a] Water Engineering and Management, School of Engineering and Technology, Asian Institute of Technology, P.O. Box 4 Klong Luang, Pathum Thani, 12120, Thailand
[b] International Water Management Institute (IWMI), Nepal Office Shree Durbar, Pulchowk, Lalitpur 3, GPO Box 8975, EPC 416, Kathmandu, Nepal

ARTICLE INFO

Keywords:
Climate change
GMS-MODFLOW
Groundwater resiliency
Kathmandu valley
RCP

ABSTRACT

Groundwater resources of Kathmandu Valley in Nepal are under immense pressure from multiple stresses, including climate change. Due to over-extraction, groundwater resources are depleting, leading to social, environmental and economic problems. Climate change might add additional pressure by altering groundwater recharge rates and availability of groundwater. Mapping groundwater resilience to climate change can aid in understanding the dynamics of groundwater systems, facilitating the development of strategies for sustainable groundwater management. Therefore, this study aims to analyse the impact of climate change on groundwater resources and mapping the groundwater resiliency of Kathmandu Valley under different climate change scenarios. The future climate projected using the climate data of RCM's namely ACCESS-CSIRO-CCAM, CNRM-CM5-CSIRO-CCAM and MPI-ESM-LR-CSIRO-CCAM for three future periods: near future (2010–2039), mid future (2040–2069) and far future (2070–2099) under RCP 4.5 and RCP 8.5 scenarios were bias corrected and fed into the Soil and Water Assessment Tool (SWAT), a hydrological model, to estimate future groundwater recharge. The results showed a decrease in groundwater recharge in future ranging from 3.3 to 50.7 mm/yr under RCP 4.5 and 19–102.1 mm/yr under RCP 8.5 scenario. The GMS-MODFLOW model was employed to estimate the future groundwater level of Kathmandu Valley. The model revealed that the groundwater level is expected to decrease in future. Based on the results, a groundwater resiliency map of Kathmandu Valley was developed. The results suggest that groundwater in the northern and southern area of the valley are highly resilient to climate change compared to the central area. The results will be very useful in the formulation and implementation of adaptation strategies to offset the negative impacts of climate change on the groundwater resources of Kathmandu Valley.

1. Introduction

Groundwater is depicted as the world's hidden treasure, constituting 94% of its freshwater resources (Koundouri and Groom, 2010). Groundwater is the most preferable source of water supply since it is of good quality and requires less treatment than surface water. In addition, the availability of groundwater is high in dry seasons than surface water and requires less investment for extraction, while its quality remains almost the same throughout the year (UK-GWF, 2018). Therefore, two billion people depend on groundwater for their daily water supply (Kemper, 2004). Groundwater resources, however, are under serious threat due to over-extraction, population growth and subsequent urbanisation, pollution and climate change/variability. It is therefore important to understand the response of the groundwater system to the aforementioned stresses to facilitate its effective management (Foster and MacDonald, 2014). Mapping groundwater resiliency, defined as the capacity of the groundwater system to withstand either long-term shocks (e.g., climate change) or short-term shocks (e.g., drought) (NGWA, 2016), can be an effective tool for understanding the groundwater system, ultimately aiding the management of groundwater resources. The term resiliency involves two main aspects of an ecosystem: the ability to resist long-term damage, and the recovery time following a disturbance (Gunderson, 2000). Resilience is often discussed in the context of climate change as the ability of a system to absorb disturbances while retaining the same basic structure and ways of functioning, and the capacity to adapt to stress and change (IPCC, 2007). Thus, groundwater resiliency is the capacity of the aquifer to absorb variable pumping stress while retaining the same basic functionality in the context of variable surface water availability and recharge, in an interrelated system. Peters et al. (2004) defined

* Corresponding author.
E-mail addresses: sangam@ait.asia, sangamshrestha@gmail.com (S. Shrestha).

https://doi.org/10.1016/j.envres.2020.109149
Received 24 November 2019; Received in revised form 15 January 2020; Accepted 16 January 2020
Available online 17 January 2020

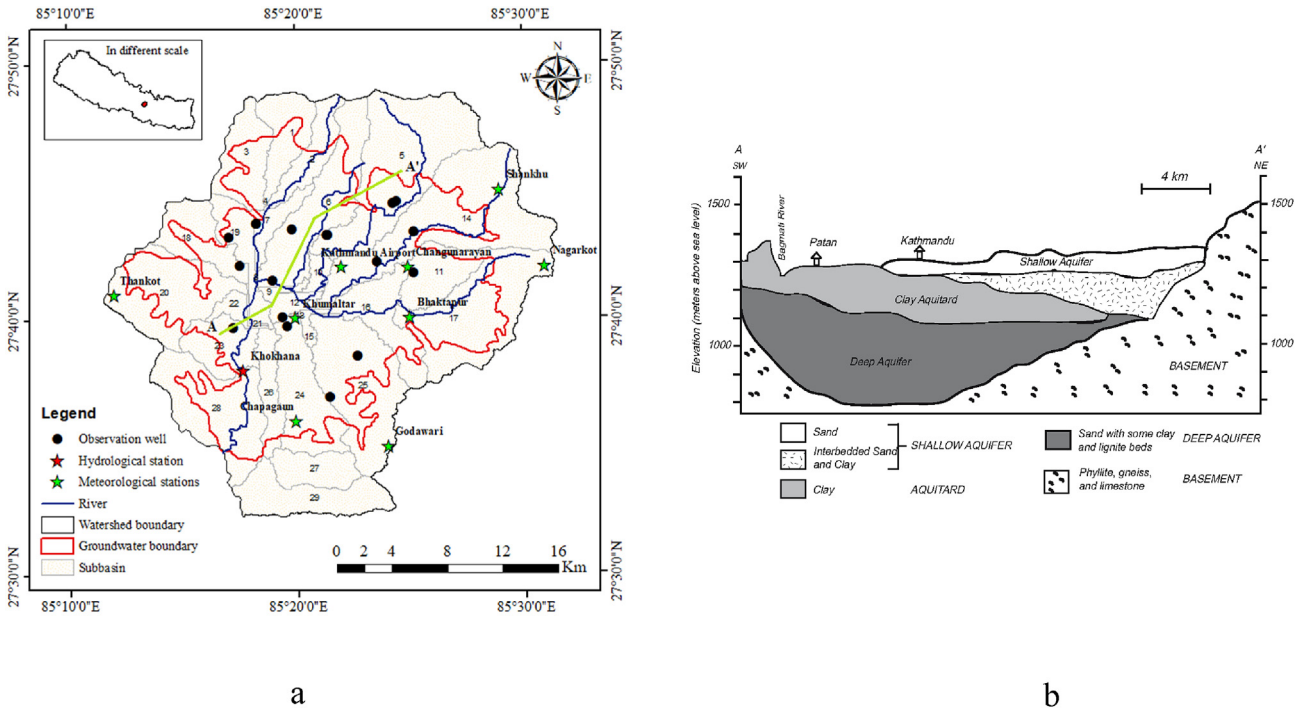

Fig. 1. Location map (a) and cross-section through the Kathmandu valley, with vertical exaggeration (Source: Jha et al., 1997; Cresswell et al., 2001) (b).

resilience as "how quickly a system is likely to recover once a failure has occurred, while vulnerability is the severity of the failure". Sharma and Sharma (2006) defined groundwater resilience as the "ability of the system to maintain groundwater reserves despite major disturbances".

The groundwater resources of Kathmandu Valley in central Nepal play a very important role in socio-economic development: providing water for domestic, agriculture and industrial purposes and the main water supply source for more than half of the population (Gautam and Prajapati, 2014). However, groundwater is under immense pressure (Pandey and Kazama, 2014) due to over-abstraction, resulting from population growth, rapid urbanisation (Pandey et al., 2010) and climate change. The global climate is changing, impacting on various sectors at different scales (Vijaya et al., 2012). The Kathmandu Valley, therefore, may not be an exception. As reported by Intergovernmental Panel on Climate Change (IPCC, 2013), the global temperature has risen by 0.3–0.6 °C and is likely to rise between 1.4 and 5.8 °C by 2100 relative to 1900. Under these circumstances, the hydrological cycle experiences significant impacts, with erratic changes in precipitation and evaporation. As this trend continues, it will seriously impact on surface and groundwater resources.

The climate change impact on groundwater depends directly on the variation in volume of its storage and circulation (Zektser and Loaiciga, 1993). Consequently, an accurate prediction of climate variables and proper estimation of groundwater recharge is essential for determining the influence of climate change in groundwater recharge. Results from various research across the globe provide sufficient evidence concerning the vulnerability of groundwater resources to climate change and consequent effects on society and ecosystems; and such studies have adopted the modelling approach to assess the impact of climate change on groundwater resources (Bates et al., 2008; Yang et al., 2010; Ali et al., 2012; Erturk et al., 2014; Shrestha et al., 2016; Pholkern et al., 2018).

A study on a small Mediterranean basin in Turkey (Erturk et al., 2014) revealed a decrease in groundwater availability as a result of climate change, indicating that water management should be treated as a primary climate change adaptation plan to address likely future water scarcity. Another study in Mekong Delta aquifers (Shrestha et al., 2016) examined the influence of climate change on groundwater resources using a hydrological model (WETSPASS), groundwater model (MODFLOW) and five Global Circulation Models (GCMs) under two Representative Concentration Pathways (RCPs) scenarios (RCP 4.5 and RCP 8.5), reporting a projected decrease in groundwater recharge as well as storage. Similarly, a study by Ali et al. (2012) focused on South-Western Australia, revealing that a decrease in rainfall in addition to groundwater over-extraction are the main reasons for declining groundwater levels and dependent ecosystems. They further found that all components of water balance like evapotranspiration, surface runoff, percolation are affected by climate change, further impacting on extractable water from both confined and unconfined aquifers. Yang et al. (2010) used rainfall-runoff model (SWAT) to estimate groundwater recharge in the Tong Zhou District, China, finding that groundwater in this region faces significant risk due to over-extraction and low rainfall. Emmanuel (2008) investigated the impact of climate change on groundwater recharge in the White Volta River Basin, Africa, revealing that shallow groundwater recharge is likely to increase remarkably under future climate change scenarios.

The aforementioned studies clearly reveal that climate change is likely to add immense pressure on groundwater resources by affecting the percolation rate and changing the availability of groundwater. However, limited studies have been conducted on groundwater in the context of climate change scenarios in the Kathmandu Valley, Nepal, and none focuses on estimating groundwater resiliency to climate change. Therefore, this research focuses on modelling and investigating the impact of climate change on groundwater resources and mapping shallow groundwater resiliency under climate change scenarios in the valley. Mapping groundwater resiliency under climate change of Kathmandu Valley can be the effective tools to identify the area where the preventive measures are urgent and to understand the behavior of groundwater system under climate change which ultimately helps in the protection and management of groundwater resources. Furthermore, it can be the effective and sustainable way to prevent the groundwater degradation by controlling over abstraction, protection of groundwater recharge area, wetlands, forest and make people understand how groundwater respond to climate change/variability.

2. Study area and data collection

2.1. Study area

Kathmandu Valley encompasses main urban cities of Nepal and situated in central Nepal (Fig. 1). The valley's watershed has an area of 656 km^2 and is enclosed within the Mahabharata hills from all sides. The groundwater basin of the valley includes three main cities: Kathmandu, Lalitpur and Bhaktapur with a total catchment area of 327 km^2. It is a closed basin with a mild slope towards the centre, and groundwater flow is presumed to be slow, mainly in the deeper aquifer (Pathak et al., 2009). The valley is surrounded by hills where the elevation is more than 2000 m a.s.l, with the central part consisting of flat land and small hills with an elevation of 1300–1400 m a.s.l. The valley has a subtropical and temperate climate with four distinct seasons: pre-monsoon (March–May), monsoon (June–September), post-monsoon (October–November) and winter (December–February). The average annual rainfall (1976–2005) in the valley is 1778 mm, the majority of which occurs during the monsoon period (June–September). The average maximum and minimum temperature (1976–2005) of the valley is 23.8 °C and 11.4 °C respectively. Bagmati, Bishnumati, Manohara, Hanumante and Dhobikhola are the major rivers in the valley.

There are two main aquifers within the unconsolidated sediments of the Kathmandu Valley, providing water to the residents (Fig. 1). The uppermost unconfined aquifer or shallow aquifer contains up to 50 m of Quaternary arkosic sand, with some discontinuous, interbedded silt and clay in Patan and Thimi formation (Yoshida and Igarashi, 1984). The uppermost shallow aquifer is underlined by aquitard, consisting of black clay with grey carbonaceous and diatomaceous beds of open lacustrine facies, reaching up to 200 m in thickness in the western part of the valley. Beneath the aquitard lies Pliocene sand-and-gravel, with interbedded lignite, peat and clay as well as the deeper confined aquifer used by several hotels, private companies and municipalities (Jha et al., 1997).

2.2. Data collection

The data used in this study includes the physical characteristics of catchment (elevation, soil and land use), time series observations (climate, hydrology, groundwater level, groundwater abstraction), hydrogeologic properties of aquifers (hydraulic conductivity (K_x, K_y), specific storage (S_s), specific yield (S_y)) and future climate projection from climate models (Table 1).

2.2.1. Historical and future climate scenarios

Historical observed climate data (1976–2005) was collected from the Department of Hydrology and Meteorology (DHM) of the Government of Nepal. Future climate projections were based on a set of Regional Climate Models (RCMs). The selection of RCMs was based on the analysis of the relationship between observed climate data and raw climate data of RCMs. In this study the climate data of following RCMs were used: ACCESS-CSIRO-CCAM, MPI-ESM-LR-CSIRO-CCAM and CNRM-CM5-CSIRO-CCAM (Table 1) under RCP 4.5 and 8.5 scenarios from the South Asia CORDEX data portal (http://cccr.tropmet.res.in/home/index.jsp) were used to derive the climate of the region in the near future (2010–2039), mid future (2040–2069) and far future (2070–2099). Representative Concentration Pathways (RCPs) scenarios depend on radiative forcing and this scenario mainly focuses on providing the concentration of greenhouse gases and radiative forcing with respect to time. Overall, there are four RCPs scenarios: RCP 2.6, RCP 4.5, RCP 6.0 and RCP 8.5 (Table 2). The main goal of the RCP scenarios is to identify future uncertainties without predicting them. These scenarios are developed using different socioeconomic hypotheses (Moss et al., 2010; Rogelj et al., 2012).

3. Methodology

The overall methodological framework adopted in this study is depicted in Fig. 2. The modelling approach was used to project future climate, groundwater recharge and groundwater level. Future climate was projected using RCM's climate data and fed into the SWAT model to simulate future groundwater recharge. The calibrated groundwater model, MODFLOW from the GMS (Groundwater Modelling System) was developed to estimate the groundwater level of the study area. Finally, the groundwater resiliency indicator was estimated based on the predicted results which in turn, was used to develop a groundwater resilience map of the study area.

DEM is a digital elevation model; LULC is land use/cover; P is precipitation; T is Temperature; RH is Relative Humidity; WS is Wind Speed; SR is Solar Radiation; Qobs is Observed River Discharge; Cal is Calibration; Val is Validation; GWLobs is Observed Groundwater Level; GW is Groundwater; RCM is a Regional Climate Model; GwRe is the groundwater resiliency; GwR is groundwater recharge; GwL is groundwater level; and n is the base year.

3.1. Future climate projection

Future climate data of RCP4.5 and 8.5 scenarios was taken from RCMs as discussed in section 2.2.1. Bias correction of climate data is usually needed because climate models often provide biased representations of observed times series due to systematic model errors which is caused by imperfect conceptualization, discretization and spatial averaging within grid cells (Teutschbein and Seibert, 2010). Meaningful bias correction is essential to avoid doubt in modelling climate change effects. According to Shrestha et al. (2017a, 2017b, 2017c), the linear scaling approach with monthly correction values based on the difference between measured and current-day computed value is sufficiently efficient to correct errors from RCM outputs on a daily time scale compared to the quantile mapping method. Hence, the linear scaling technique was selected for this study since it is simple and has been applied in several studies (Shrestha et al., 2017a, 2017b, 2017c).

RCMs precipitation was corrected based on the proportion of long-term mean observed and control data as given in equations (1) and (2). RCMs temperature was corrected using an additive term obtained from the difference between the measured long-term monthly mean and control data as given in equations (3) and (4).

$$P_{his}(d)^* = P_{his}(d)[\mu_m\{P_{obs}(d)\}/\mu_m\{P_{his}(d)\}] \quad (1)$$

$$P_{sim}(d)^* = P_{sim}(d)[\mu_m\{P_{obs}(d)\}/\mu_m\{P_{his}(d)\}] \quad (2)$$

$$T_{his}(d)^* = T_{his}(d) + [\mu_m\{T_{obs}(d)\} - \mu_m\{T_{his}(d)\}] \quad (3)$$

$$T_{sim}(d)^* = T_{sim}(d) + [\mu_m\{T_{obs}(d)\} - \mu_m\{T_{his}(d)\}] \quad (4)$$

where, P is precipitation, T is temperature, d is daily, μ_m is the long-term monthly mean, (*) represents bias corrected, *his* refers to historical raw RCM data, *obs* refers to observed data and *sim* is the raw RCM future data.

The bias-corrected future time series was then used to analyse projected future climate change w.r.t. baseline in terms of long-term average, seasonal variations in change, changes across different future periods, and variation in changes with RCP scenarios.

3.2. Hydrological model development

The hydrological model for the Kathmandu Valley watershed was developed using the Soil and Water Assessment Tool (SWAT), which is a physically based, semi-distributed hydrological model used extensively for studying different water quality and hydrological problems in various watersheds under different management practices (Luo et al., 2008). The SWAT model is also considered to be a classic instrument in

Table 1
Data used in this study and corresponding sources of data.

SN	Data	Source/Developer	Spatial/Temporal Resolution	Time Period	
Physical characteristics of the catchment					
1	Elevation	ASTER GDEM	30 m/-	–	
2	Soil	SOTER, Nepal	30 m/-	2010	
3	Land Use	ICIMOD, Nepal	30 m/-	2010	
Time series observation					
1	Meteorology	DHM, Nepal	Point/Daily	1976–2005	
2	Hydrology	DHM, Nepal	Point/Daily	1976–2005	
3	Groundwater Level	GWRDB, Nepal	Point/Yearly	2001 and 2008	
4	Groundwater Abstraction	DHM, Nepal	Point/Yearly	2001 and 2008	
Hydrogeologic properties					
1	Hydraulic conductivity (K_x, K_y)	Pandey and Kazama (2011)	1 per aquifer layer	–	
2	Specific storage (S_s)	Pandey and Kazama (2011)	1 per aquifer layer	–	
3	Specific Yield (S_y)	Pandey and Kazama (2011)	1 per aquifer layer	–	
RCMs data for future climate projection					
SN	Data	Source/Developer	Spatial/Temporal Resolution	Parent GCM	RCP/Time Period
1	ACCESS-CSIRO-CCAM	Collaboration for Australia Weather and Climate Research, Australian Government	0.5°/Daily	ACCESS1.0	RCP 4.5 and RCP 8.5: 1975–2099
2	MPI-ESM-LR-CSIRO-CCAM	National Center for Meteorological Research	0.5°/Daily	CNRM-CM5	RCP 4.5 and RCP 8.5: 1975–2099
3	CNRM-CM5-CSIRO-CCAM	European Network for Earth System Modelling	0.5°/Daily	MPI-ESM-LR	RCP 4.5 and RCP 8.5: 1975–2099

Note: SOTER: Soil and Terrain. ICIMOD: International Centre for Integrated Mountain Development. DHM: Department of Hydrology and Meteorology. RCP: Representative Concentration Pathways. GWRDB: Groundwater Resources Development Board. ASTER GDEM: Advanced Spaceborne Thermal Emission and Reflection Radiometry Global Digital Elevation Model.

spatial decision support systems (Cibin et al., 2010). In this study, the SWAT was used to evaluate the groundwater recharge since it has been broadly used by hydrologists since 1993 for studying various problems in watershed hydrology (Santhi et al., 2001; Alansi et al., 2009; Piman et al., 2013; Arias et al., 2014; Yen et al., 2015; Shrestha et al., 2017a,2017b,2017c; Pandey et al., 2019). The hydrological simulation in SWAT is based on the following water balance equation:

$$SW_t = SW_0 + \sum_{i=1}^{t} (R_{day} - Q_{surf} - E_a - W_{seep} - Q_{gw}) \quad (5)$$

where, SW_t is the soil water content (mm water) at the end of time step t (days), SW_0 is the initial soil water content in day i (mm water), R_{day} is the amount of precipitation on day i (mm water), Q_{surf} is the amount of surface runoff on day i (mm water), E_a is the amount of evapotranspiration on day i (mm water), W_{seep} is the amount of water entering the vadose zone from the soil profile on day i (mm water), Q_{gw} is the amount of base flow from the shallow aquifer on day i (mm water).

The SWAT model for this study was set up by discretising the Kathmandu Valley watershed into 29 sub-basins and 220 hydrological response units (HRUs) based on drainage density. As the computational blocks of the SWAT model, HRUs are located in the sub-watershed and respond similarly to the given inputs such as temperature and rainfall. The HRUs in the SWAT are classified according to land cover, soil type and slope. The slope of the basin was classified into four classes; 0–22%, 22–48%, 48–80% and 80–99% with the HRUs developed by fixing a 5% threshold for each land use percentage over the sub-basin area, soil class percentage over the land use area and slope class percentage over the soil area. Six years (1996–2001) of flow data for the Bagmati River at Khokhana station (550.5) (Fig. 1) was used for calibration and four years (2002–2005) of flow data for validation. The model was calibrated and validated for daily time scale. The model performance was evaluated by visually comparing observed and simulated hydrographs with values calculated using Nash-Sutcliffe Efficiency (NSE), Percent Bias (PBIAS) and Coefficient of Determination (R^2). In equations, Q_m is the modelled discharge (m^3/s); Q_o - observed discharge (m_3/s); N or T is number of data points.

$$NSE = 1 - \frac{\sum_{t=1}^{T} (Q_m^t - Q_o^t)^2}{\sum_{t=1}^{T} (Q_o^t - \bar{Q}_o)^2} \quad (6)$$

$$PBIAS = 100 \frac{\sum_{t=1}^{T} Q_m^t - Q_o^t}{\sum_{t=1}^{T} Q_o^t} \quad (7)$$

$$R^2 = \left(\frac{\sum_{t=1}^{N} (Q_o^t - \bar{Q}_o)(Q_m^t - \bar{Q}_m)}{\sqrt{\sum_{t=1}^{N} (Q_o^t - \bar{Q}_o)^2} \sqrt{\sum_{t=1}^{N} (Q_m^t - \bar{Q}_m)^2}} \right)^2 \quad (8)$$

3.3. Groundwater flow model development

The groundwater model, MODFLOW from the GMS, was used to simulate the groundwater level in the valley's aquifers. The MODFLOW model is one of the most widely used groundwater model across the globe and a flexible groundwater modelling tool for examining the dynamics of groundwater systems and interpreting flow patterns.

Table 2
Brief description of RCP scenarios (Source: Moss et al., 2010).

RCP	Description	CO_2 Equivalence (ppm)	Temperature Anomaly (°C)
RCP 2.6	Peak in radiative forcing at ~ 3 W/m^2 before 2100 and decline	490	1.5
RCP 4.5	Stabilisation without overshoot pathways to 4.5 W/m^2 at stabilisation after 2100	650	2.4
RCP 6.0	Stabilisation without overshoot pathways to 6 W/m^2 at stabilisation after 2100	850	3.0
RCP 8.5	Rising radiative forcing pathways leading to 8.5 W/m^2 in 2100	1370	4.9

Notes: RCP is the Representative Concentration Pathway.

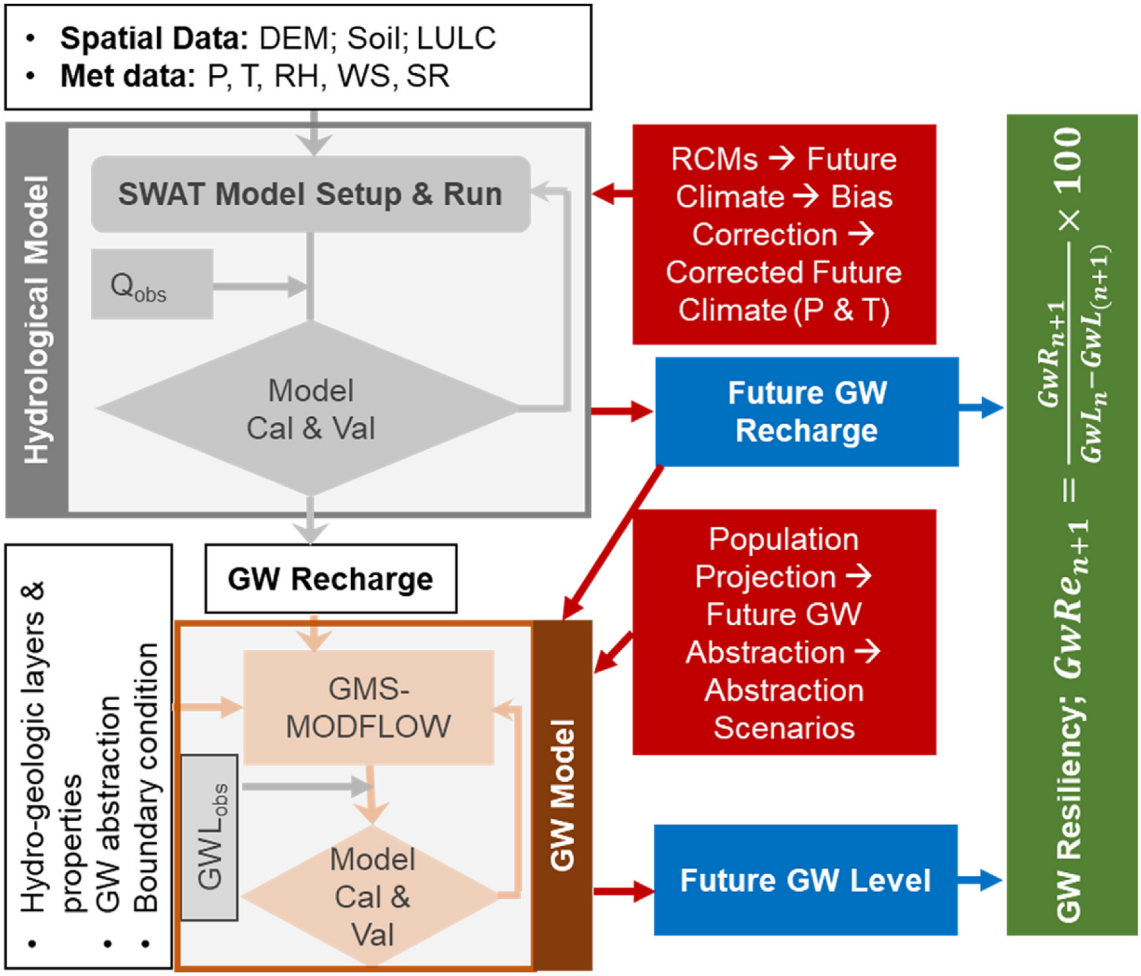

Fig. 2. Groundwater resiliency mapping — Methodological Framework.

Furthermore, this model is also used as a tool for estimating recharge, aquifer storage processes, discharge as well as enumerating sustainable yield (Zhou and Li, 2011). In addition, the MODFLOW model has been extensively used by many researchers and hydrogeologists to simulate the flow of groundwater through the aquifers (Yang et al., 2010; Ali et al., 2012; Lachaal et al., 2012; Cheng et al., 2013; Maheswaran et al., 2016).

The three-dimensional groundwater flow through the porous medium is governed by the following equation:

$$\frac{\partial}{\partial x}\left(K_x \frac{\partial h}{\partial x}\right) + \frac{\partial}{\partial y}\left(K_y \frac{\partial h}{\partial y}\right) + \frac{\partial}{\partial x}\left(K_z \frac{\partial h}{\partial z}\right) = S_s \frac{\partial h}{\partial z} - W \quad (9)$$

where, K_x, K_y, K_z are the values of hydraulic conductivity along x, y and z axes [LT^{-1}], h is the hydraulic head [L], W is flux per unit volume, representing sink and/or sources of water [T^{-1}], S_s is the specific storage of the aquifer [L^{-1}].

Equation (9) describes the transient flow when combined with both the initial and boundary conditions and steady state, while the term in the right side of the equation is assumed to be zero. Flow area in the MODFLOW is represented by grids and layers. Each grid and layer is expected to have consistent properties and Equation (9) is used to calculate the head of the layer. For confined layers, the head can rise above the top elevation while the simulated head remains below the surface of the unconfined layer.

The GMS-MODFLOW model was set up by discretising a groundwater basin of 327 km^2 into 52 rows and 58 columns with a cell size of 500 m × 500 m enclosed in modified UTM coordinates of 618810.4 m–646528 m east and 3051038 m to 3076021 m north. The inside grid of the groundwater border was set as an active area and the outside grid an indolent or inactive area. Vertically, the grids are alienated into three layers; the shallow aquifer (unconfined aquifer) as the topmost layer, aquitard (non-simulated layer) as the middle layer and the deep aquifer (confined aquifer) as the lowermost layer. Model inputs include the elevation of each layer, hydrogeological properties, boundary conditions, initial groundwater levels, recharge and discharge. Kathmandu Valley is separated by a rock surface on all sides and was, therefore, assumed to be a no-flow boundary, meaning that groundwater fluxes across the boundary will not occur. The groundwater level data for 18 observation wells and pumping data for 258 Kathmandu Upatyaka Khanepani Limited (KUKL) pumping wells were used in the model. The total groundwater abstraction was reported to be 21.26 million cubic metres (MCM) in 1999 and 25.52 MCM in 2009 (Pandey and Kazama, 2014). However, there is no exact number for pumping wells in operation. It is observed that most of the pumping wells in Kathmandu Valley are distributed in the central area. Groundwater level data for 18 observation wells in 2001 was used for model calibration with 2008 used for model validation. The model simulation was conducted in the steady-state condition to obtain future groundwater levels. The hydraulic properties of the Kathmandu aquifer system are summarised in Table 3.

3.4. Climate change impact assessment

To assess the climate change impact, SWAT model and GMS-MODFLOW inputs were analysed according to the projected future climate. Any changes in recharge areas and groundwater levels through

Table 3
Hydraulic properties of the Kathmandu aquifer system (Source: Pandey and Kazama, 2011).

S. N	Parameters	Shallow Aquifer	Deep Aquifer
1	Surface Area, A (km^2)	241	327
2	Transmissivity, T (m^2/day)	163.2–1056.6	22.6–737
3	Hydraulic Conductivity, K (m/day)	12.5–44.9	0.3–8.8
4	Permeability, k (m^2)	1.48E-11 to 5.32E-11	3.74E-13 to 1.04E-11
5	Storage Coefficient, S	0.2	0.00023–0.07
6	Total Aquifer Volume (MCM)	7261.27	56813.7

Table 4
Per capita water demand by category for Kathmandu Valley, Nepal (Source: Udmale et al., 2016, Bureau of Indian Standard, IS 1172: 1993, Code of Basic Requirements for Water Supply, Drainage and Sanitation and expert suggestion).

Category	Litres per capita per day
Domestic demand	135
Public demand (water demand for public utility purposes such as the washing of public parks and roads, gardening, public fountains)	20
Industrial demand	50
Commercial demand	20
Fire demand	15
Loss and waste	50
Total	270

input changes, with respect to the baseline values, were taken as impacts of climate change. Baseline values for groundwater recharge and its spatial distribution were estimated from the calibrated/validated SWAT model. Similarly, the baseline value of the groundwater level was estimated from the calibrated/validated GMS-MODFLOW.

3.5. Population projection and future groundwater abstraction estimation

The population of the valley has already come to saturation points because the hill surrounding it acts as a fence against further increment. Hence, the logistic curve method was used for forecasting the population of Kathmandu Valley (Shrestha et al., 2017). This method accepts that population trails the growth curve features within partial space and economics. Firstly, the city's population rises at a very slow rate and then expands rapidly in certain periods before declining again, thus creating an S-curve which is called the logistic curve.

$$P_t = \frac{P_{sat}}{1 + e^{(a+b\Delta t)}} \tag{10}$$

$$P_{sat} = \frac{2P_0P_1P_2 - P_1^2(P_0 + P_2)}{P_0P_2 - P_1^2} \tag{11}$$

$$a = \ln\left(\frac{P_{sat} - P_0)}{P_0}\right) \tag{12}$$

$$b = \frac{1}{n}\ln\frac{P_0(P_{sat} - P_0)}{P_1(P_{sat} - P_0)} \tag{13}$$

where, P_0, P_1, P_2 = population at time period 1991, 2001 and 2011 respectively (CBS, 1991, 2001, 2011), P_{sat} = population at saturation level, Δt = number of years after base year, a, b = data constants, n = time interval between successive years.

Per capita water demand for Kathmandu Valley was assumed to be 270 L per day. Hence, the water demand was determined by multiplying the projected population by litres per capita per day (lpcd), as categorised in Table 4.

To calculate future groundwater abstraction, the following three scenarios were analysed:

- Scenario 1 (S1): 20% of the total water demand is fulfilled by groundwater abstraction
- Scenario 2 (S2): 35% of the total water demand is fulfilled by groundwater abstraction
- Scenario 3 (S3): 50% of the total water demand is fulfilled by groundwater abstraction

Different studies reveal that groundwater is the main source of water supply in Kathmandu valley, Nepal (Gautam and Prajapati, 2014). Kathmandu Upatyaka Khanepani Limited (KUKL) is the only water supply operator providing water supply services in the urban and rural areas of the valley (Shrestha, 2012). In total, KUKL supplies 22.5% of the total water demand in the driest month and up to a maximum of 37.8% in the wettest month (KUKL, 2011). The portion of groundwater contribution is 35% in dry season and 11% in wet season with a yearly average of 19% in 2011 (KUKL, 2011).

The scenario 1 (S1) in this study assumes 20% of total water demand is fulfilled by groundwater abstraction and is the optimistic scenario which designate the reduction in groundwater abstraction for the implementation of policies to prevent groundwater abstraction or trans boundary water diversion from different river basin.

In our study, groundwater abstraction data for 258 KUKL operated pumping wells of year 2001 and 2008 were used. Since there were no exact numbers of private wells for commercial, industrial, agricultural and household purposes, we assumed that 35% of the total water demand is fulfilled from groundwater abstraction (19% from KUKL well and 16% from private wells for commercial, industrial, agricultural and household purposes).

Therefore, scenario 2 (S2) assumes that 35% of the total water demand is fulfilled by groundwater abstraction as in business as usual scenario.

The scenario 3 (S3) assumes that 50% of the total water demand is fulfilled by groundwater abstraction and is the pessimistic scenario where the groundwater abstraction further increases in future.

3.6. Groundwater resiliency mapping

Groundwater resiliency to climate change in this study is defined as the percentage recovery to the total depletion of groundwater level at a given time and can be described as follows:

Table 5
Groundwater resiliency classification and its interpretation.

Groundwater Resiliency (GwRe) Value (%)	Resiliency Class	Interpretation
0 to 1	Not resilient	Less groundwater recharge, higher reduction of groundwater level
1 to 3	Fairly resilient	Less groundwater recharge, fair reduction of groundwater level
3 to 5	Moderately resilient	Moderate groundwater recharge, moderate reduction of groundwater level
5 to 8	Highly resilient	Higher groundwater recharge, less reduction of groundwater level
> 8	Very highly resilient	Higher groundwater recharge and very less reduction of groundwater level

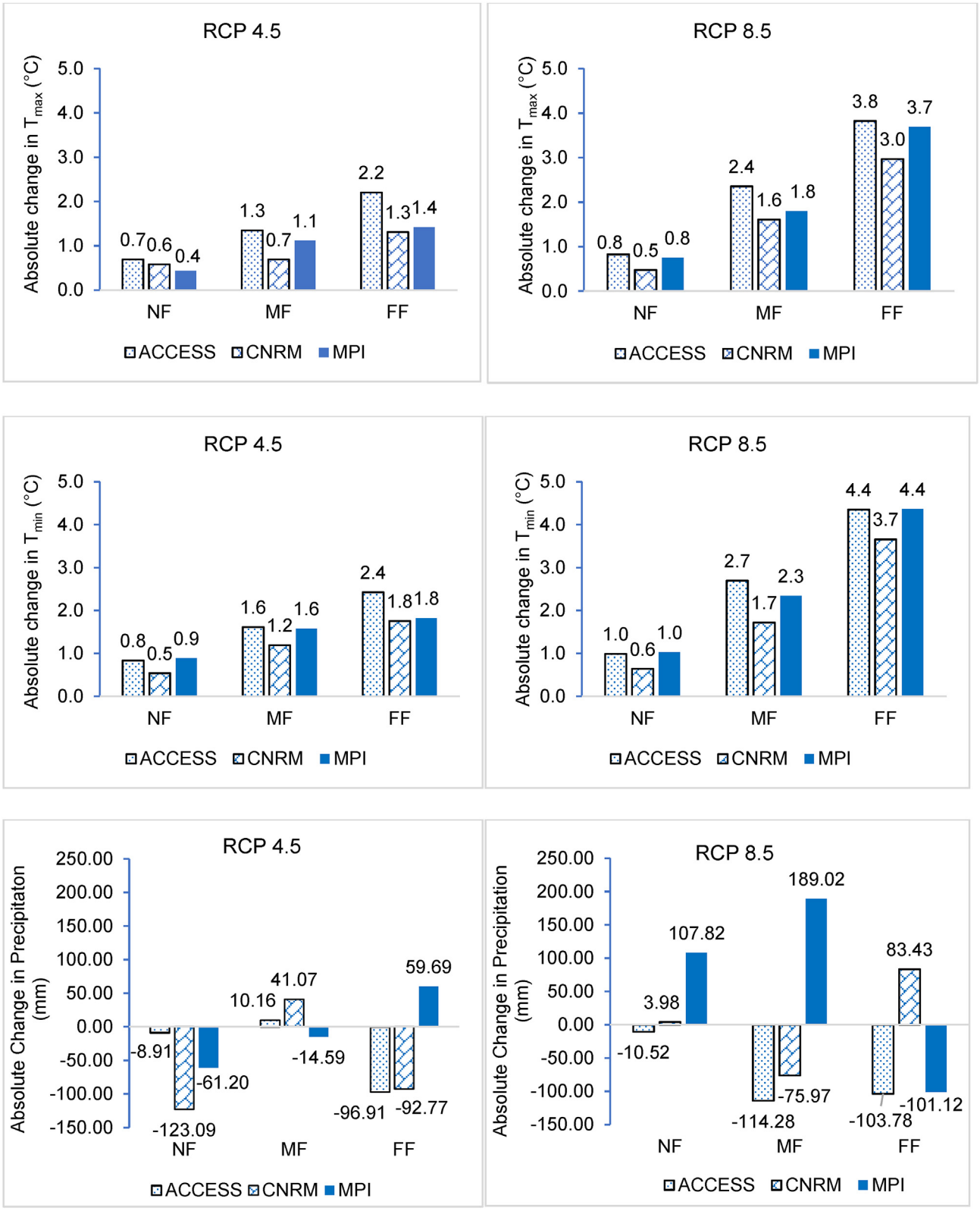

Fig.3. Absolute change in maximum temperature (top), minimum temperature (middle) and precipitation (bottom) for the three future periods: NF (2010–2039), MF (2040–2069) and FF (2070–2099) relative to the baseline period (1976–2005) under RCP 4.5 and RCP 8.5 scenarios.

$$GwRe_{n+1} = \frac{GwR_{(n+1)}}{GwL_n - GwL_{(n+1)}} \times 100 \quad (16)$$

where, n represents the base year, GwRe is groundwater resiliency, GwR is groundwater recharge and GwL is groundwater level.

Groundwater resiliency (GwRe) was further divided into five different classes to develop a groundwater resiliency map of Kathmandu Valley (Table 5). Equation (16) shows that, groundwater resiliency for the particular year depends directly on the groundwater recharge of that year and inversely to the change in groundwater level between that

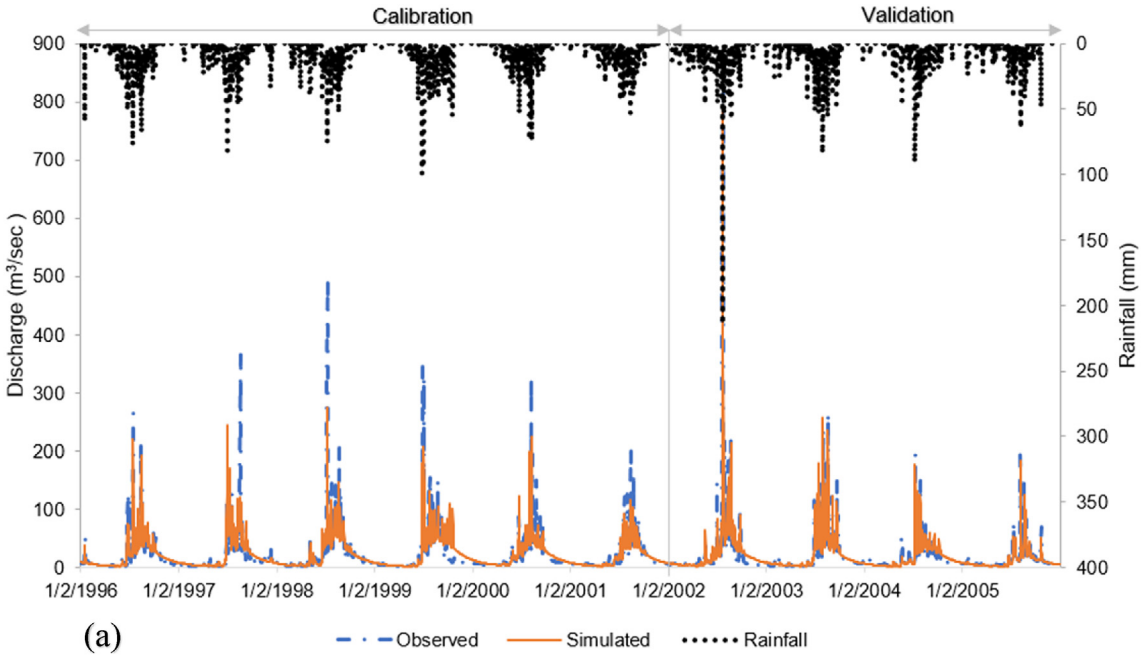

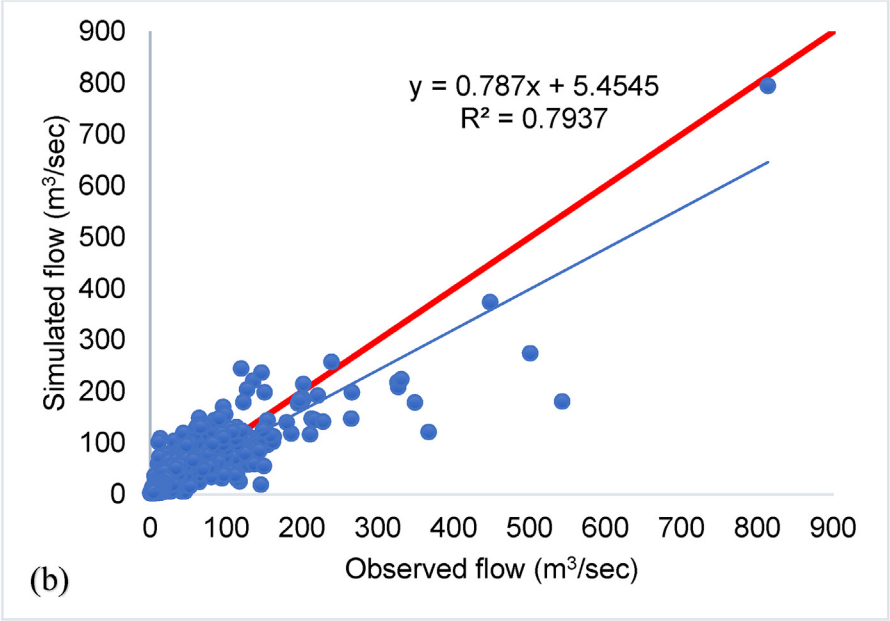

Fig. 4. Hydrograph at Khokana station (550.5) showing the results of calibration for the period 1996–2001 and validation for the period 2002–2005 (a), observed vs simulated flow during the calibration period 1996–2001 and validation period 2002–2005 (b) (red line resembles the 45-degree line and blue line resembles the line of best fit or trendline). (For interpretation of the references to colour in this figure legend, the reader is referred to the Web version of this article.)

particular year and base year. Higher the percentage of recovery over total depletion, higher will be the groundwater resiliency.

Groundwater system is very highly resilient, if the groundwater level increases in future. Also, for higher groundwater recharge and lesser reduction in groundwater level, groundwater system is be highly resilient (decrease in groundwater level is less than 20 times the groundwater recharge). Similarly, for lesser groundwater recharge and higher reduction in groundwater level, groundwater system is not resilient (decrease in groundwater level is greater than 100 times the groundwater recharge).

4. Results and discussion

4.1. Projected future climate of Kathmandu Valley

Future climate is described by change in temperature (T_{max}, T_{min}) and precipitation using RCM (CSIRO-CCAM), but driven by three different GCMs); ACCESS-CSIRO-CCAM, MPI-ESM-LR-CSIRO-CCAM and CNRM-CM5-CSIRO-CCAM under two emission scenarios (RCP 4.5 and RCP 8.5) for the near future (2010–2039) mid future (2040–2069) and far future (2070–2099). This includes comparing the baseline (1976–2005) climate datasets with bias-corrected climate datasets. The linear scaling method was used to remove bias from the climate model outputs. The R^2, RMSE and standard deviation (SD) values were also

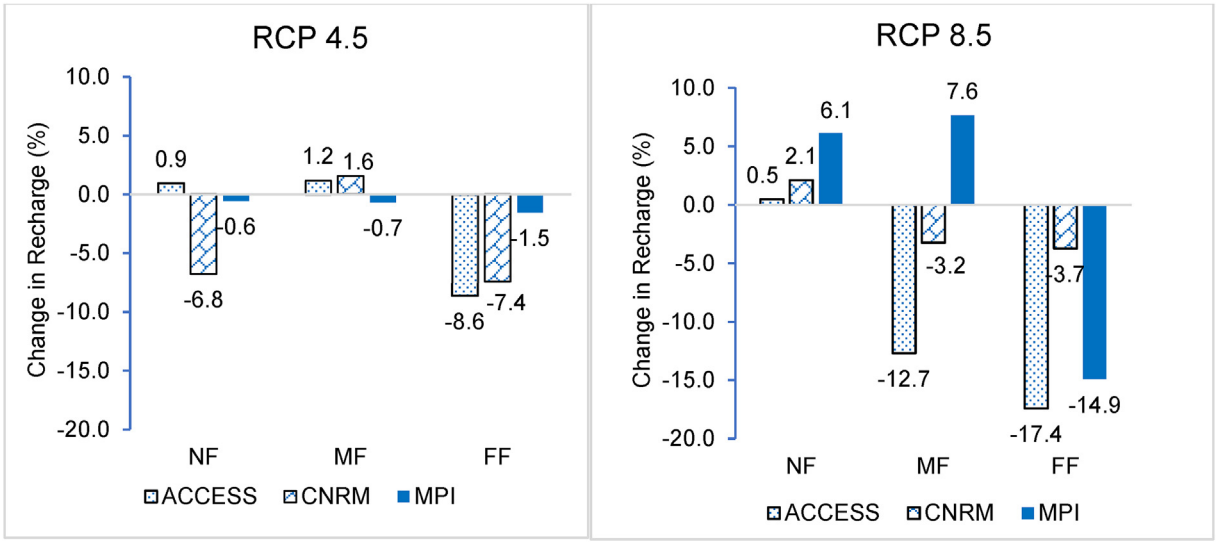

Fig. 5. Relative change in groundwater recharge for the Kathmandu Valley during three future periods: NF (2010–2039), MF (2040–2069), FF (2070–2099) under RCP 4.5 and RCP 8.5 scenarios in respect to baseline recharge (1996–2005).

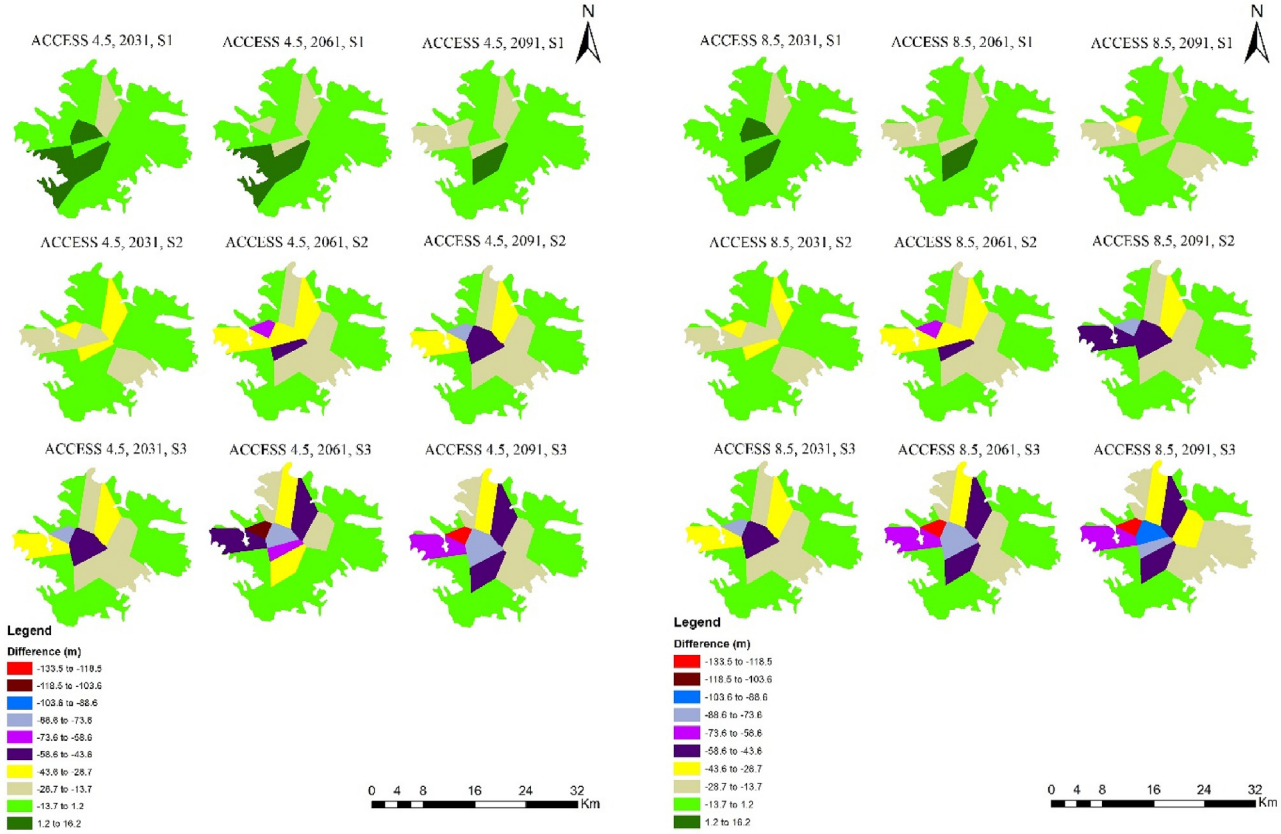

Fig. 6. Relationship between observed head (masl) and simulated head (masl) in the steady-state condition for calibration period (a) and validation period (b).

calculated to check the accuracy of the bias corrected data. The results reveal the betterment in R^2 and minimisation of SD and RMSE values after bias correction (Table S1). Supplementary Table S1 shows the summary statistics for the performance of ACCESS-CSIRO-CCAM RCM. However, performance of the other RCMs was also similar.

The annual average baseline precipitation, T_{max}, and T_{min} of Kathmandu Valley was 1778 mm, 23.8, and 11.4 °C, respectively. All RCMs and both RCP scenarios indicated that T_{max} and T_{min} are projected to increase in the future. The projected increase in T_{max} ranges from 0.4 to 2.2 °C in RCP 4.5 scenario and 0.5–3.8 °C in RCP 8.5. Similarly, the projected increase in T_{min} ranges from 0.5 to 2.4 °C in RCP 4.5 scenario and 0.6–4.4 °C in RCP 8.5. The ACCESS-CSIRO-CCAM RCM projected maximum increases in future maximum and minimum temperatures in the near, mid and far future for both RCPs scenarios. The increase in T_{min} was found to be considerably higher than that of T_{max} (Vose et al., 2005; Kharin et al., 2013). Fig. 3 (top and middle) shows the absolute change in temperature with respect to the baseline period.

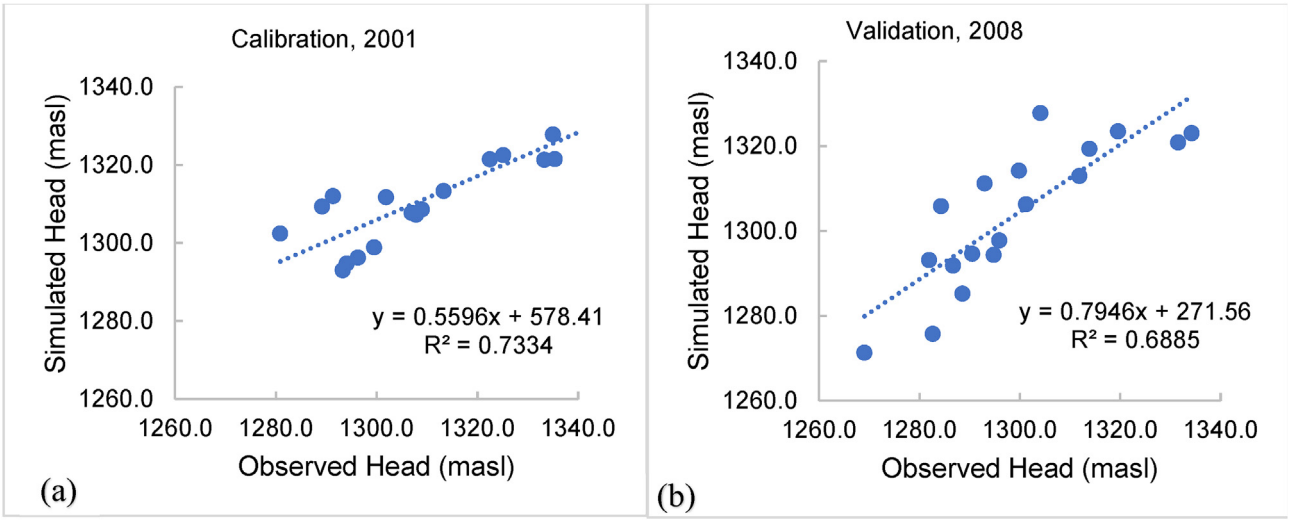

Fig.7. Average change in groundwater level for all three RCMs (ACCESS-CSIRO-CCAM, MPI-ESM-LR-CSIRO-CCAM and CNRM-CM5-CSIRO-CCAM), both RCP scenarios (RCP 4.5, RCP 8.5) and three pumping scenarios (S1, S2 and S3) for three future periods: 2031, 2061 and 2091 relative to the baseline (2001).

Precipitation is projected to vary throughout the future. The ACCESS-CSIRO-CCAM RCM shows that precipitation during the future period is expected to decrease in both RCP 4.5 and RCP 8.5 scenarios. The ACCESS-CSIRO-CCAM RCM projected a maximum decrease in future precipitation of 114.28 mm in the mid future under RCP 8.5 scenario, while CNRM-CM5-CSIRO-CCAM shows a maximum decrease in future precipitation of 123.09 mm in the near future under RCP 4.5. The MPI-ESM-LR-CSIRO-CCAM RCM projected a maximum increase in future precipitation of 59.69 mm in the far future under RCP 4.5 scenario and 189.02 mm in the mid future under RCP 8.5. Average precipitation during the post-monsoon, pre-monsoon and winter seasons is expected to increase by a certain amount, whereas the result shows a significant decrease during the monsoon period for both climate change scenarios. Fig. 3 (bottom) shows the absolute change in future precipitation with respect to the baseline period. With the exception of ACCESS-CSIRO-CCAM RCM, the other two RCMs project future precipitation in a random manner without a clear increasing or decreasing pattern in the projected precipitation values. This somehow explains the uncertainty which could potentially arise from these inputs in terms of hydrological simulation for future conditions. This is the main reason for selecting data on more than one RCM to assess the impact of climate on hydrological processes in the future.

4.2. SWAT model calibration and validation

Calibration and validation of the SWAT model was conducted for daily streamflow at the basin outlet at Khokana station (550.5). Six years (1996–2001) of flow data was used for calibration and four years (2002–2005) for validation. For auto calibration, SWAT-CUP was used. The calibration process includes identifying sensitive parameters. The sensitivity analysis of the parameters was carried out to analyse the effect of an incremental change in input parameters on the corresponding change in output values. About 31 parameters were used for sensitivity analysis which are GWQMN.gw, SOL_ALB().sol, GW_REVAP.gw, SURLAG.bsn, CH_S1.sub, ESCO.hru, GW_SPYLD.gw, LAT_TIME.hru, GDRAIN.mgt, CH_N1.sub, EPCO.hru, SOL_BD().sol, CANMX.hru, REVAPMN.gw, CH_K2.rte, ICN.bsn, SOL_K().sol, SHALLST.gw, DEEPST.gw, SLSOIL.hru, SOL_AWC().sol, CNCOEF.bsn, OV_N.hru, SLSUBBSN.hru, CH_K1.sub, ALPHA_BF.gw, GW_DELAY.gw, CN2.mgt, RCHRG_DP.gw, CH_W1.sub and CH_L1.sub. Out of 31 parameters, 23 parameters are selected for model calibration which are listed in Supplementary Table S2 with their sensitivity rank. The accuracy of the model was tested by checking the fitness of the observed and simulated flow values (Fig. 4). In addition, statistical performance indicators such as NSE, PBIAS and R^2 were calculated for both calibration and validation periods. The NSE was used as the objective function and the threshold value was set at 0.5. The NSE, R^2 and PBIAS values for calibration were 0.75, 0.76 and −5.49, respectively, and 0.83, 0.84 and −9.53 for validation. This shows that the prediction performance of the model is reasonably good, thus, the validated model can realistically be used for future predictions. The performance of the model is good in daily time-steps for calibration and validation periods (Moriasi et al., 2007).

4.3. Impact of climate change on groundwater recharge

Groundwater recharge for the three future periods: near future (2010–2039) mid future (2040–2069) and far future (2070–2099) and the two RCPs scenarios (RCP 4.5 and RCP 8.5) were compared with the baseline (1996–2005) groundwater recharge of 587.03 mm/year. In similarity to the precipitation pattern, groundwater recharge is projected to be highly erratic throughout the future for almost all RCMs. The ACCESS-CSIRO-CCAM RCM projected a maximum decrease in groundwater recharge of 8.6% in the far future under RCP 4.5 scenario and 17.4% for the far future under RCP 8.5. The MPI-ESM-LR-CSIRO-CCAM RCM shows a maximum increase in groundwater recharge of 7.6% in the mid future under RCP 8.5 scenario while CNRM-CM5-CSIRO-CCAM RCM projected a maximum increase in groundwater recharge of 1.6% in the mid future under RCP 4.5. The average groundwater recharge during post-monsoon, pre-monsoon and winter seasons is projected to increase by a certain amount with respect to precipitation. However, the compelling results show a projected decrease in groundwater recharge during the monsoon season. The decrease in monsoon groundwater recharge ranges from 1.05 to 16.38% in RCP 4.5 scenario and 0.23–20.29% in RCP 8.5. Since more than 80% of the precipitation in Kathmandu Valley occurs during the monsoon season, the decrease in monsoon groundwater recharge is more significant. Fig. 5 shows the change in groundwater recharge relative to the baseline. The projected change in groundwater recharge under climate change scenarios is shown in Supplementary Table S3.

4.4. Calibration and validation of groundwater model

A steady-state groundwater model was developed for 2001. To achieve good agreement between the simulated and observed hydraulic heads, the values of hydraulic conductivities in each layer were

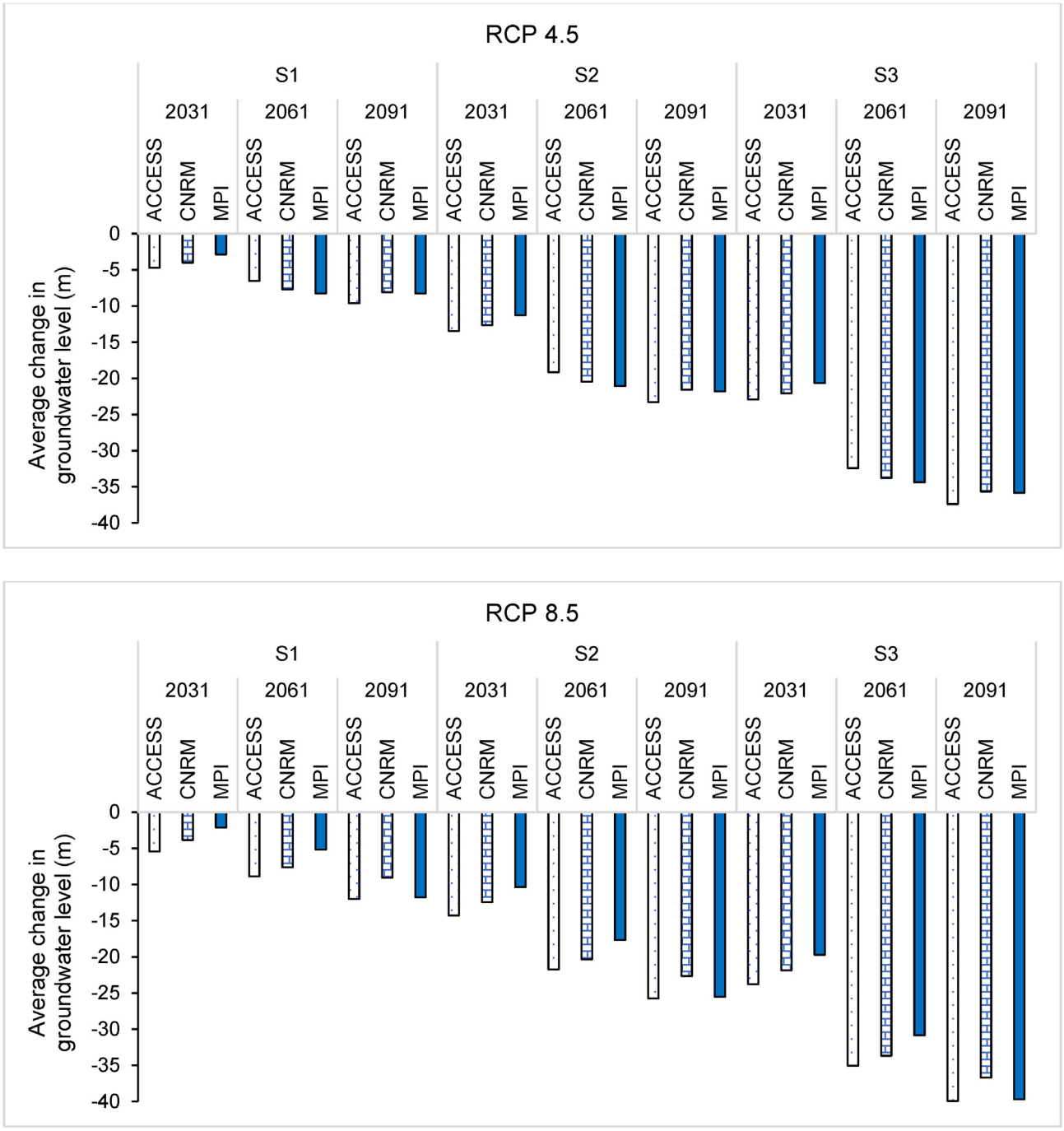

Fig. 8. Change in future groundwater level with respect to the observed baseline groundwater level (2001) for three different time periods: 2031, 2061 and 2091 with S1, S2 and S3 in respect of ACCESS-CSIRO-CCAM RCM and RCPs 4.5 and 8.5 scenarios.

adjusted within the acceptable limits. Model calibration was conducted by the trial and error method, and after several runs, the values of hydraulic conductivities in different layers were adjusted until a good match was achieved between observed and simulated heads. In addition, adjustments were also made to the river conductance and depth for model calibration. Hydraulic conductivity was found to be 40 m/day, 40 m/day and 4 m/day in x, y and z direction respectively for the shallow aquifer, 3 m/day, 3 m/day and 0.3 m/day in x, y and z direction respectively for the deep aquifer and 0.006048 m/day, 0.006048 m/day and 0.0006048 m/day in x, y and z direction respectively for the aquitard. The average river depth of 0.4 m used for calibration. The model was validated for 2008, keeping the same calibration parameter and only changing the input data such as groundwater recharge, groundwater abstraction and observed groundwater levels. The model performance was evaluated using R^2 as a statistical measure. The R^2 value for the calibration period was found to be 0.73 with 0.68 for the validation period. This suggests that the overall performance of the model is fairly good. The relationship between observed and simulated heads for both calibration and validation periods are shown in Fig. 6. The model results for observed and simulated heads in the steady-state condition, calibration period (2001) and validation period (2008) are shown in Supplementary Table S4.

4.5. Impact of climate change on the groundwater level

The impact of climate change on the groundwater level was

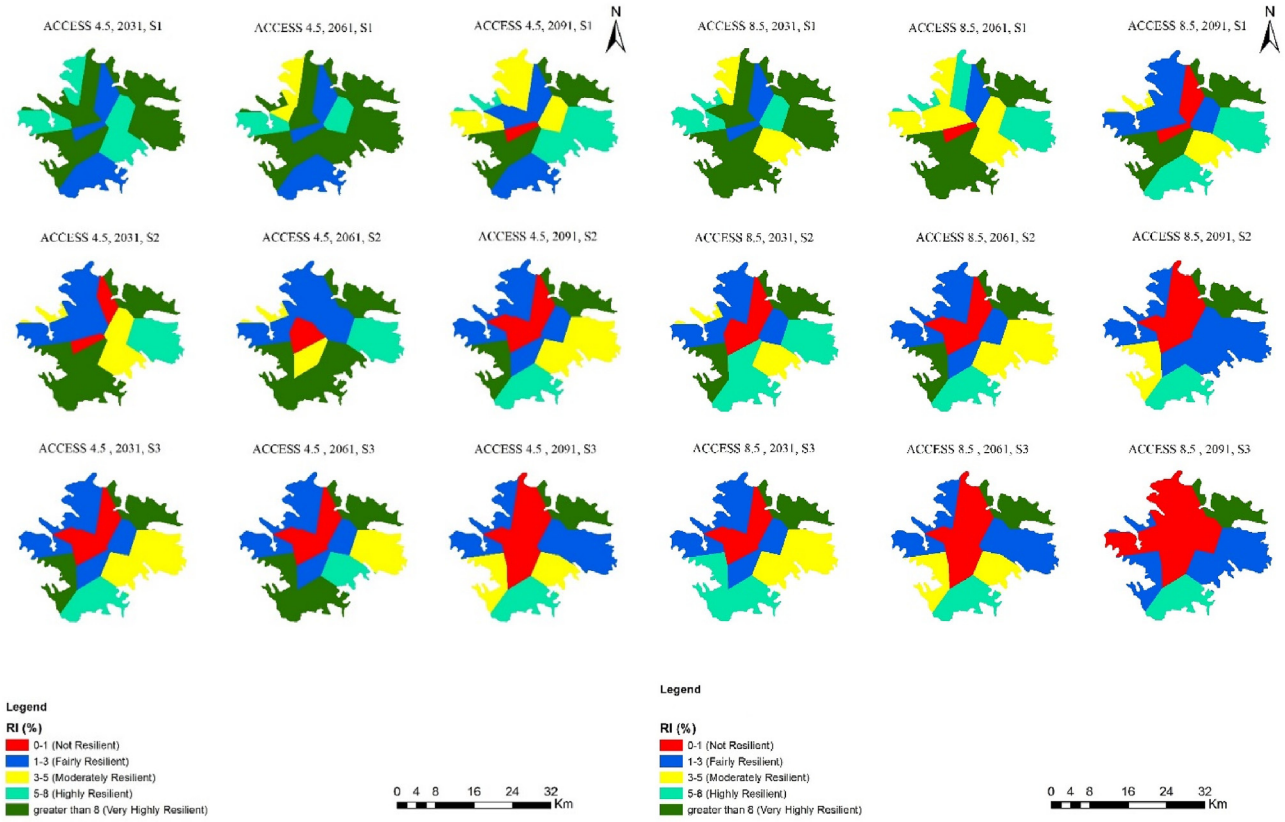

Fig. 9. Groundwater resiliency map of Kathmandu Valley, Nepal for three different time periods: 2031, 2061 and 2091 with Scenarios S1, S2 and S3 for ACCESS-CSIRO-CCAM RCM and RCP 4.5 and RCP 8.5 scenarios.

projected for three future periods: 2031, 2061 and 2091 under two RCPs scenarios (RCP 4.5 and RCP 8.5) after comparison with the baseline (2001). Three pumping scenarios were also analysed to calculate future groundwater abstraction, and subsequently used to calculate future groundwater levels. Pumping scenarios S1, S2 and S3 indicate that 20, 35 and 50% of the total water demand is fulfilled by groundwater abstraction, respectively.

All RCMs and both RCP scenarios project that, on average, the groundwater level will decrease in future for all three pumping scenarios: S1, S2 and S3 (Fig. 7). The average decrease in groundwater level was higher for scenario S3 than S2 and S1. The ACCESS-CSIRO-CCAM projects a maximum decrease in the average groundwater level of 9.6 m for pumping scenario S1, 23.2 m in S2 and 37.4 m in S3 for RCP 4.5 scenario and 12 m for S1, 25.8 m for S2 and 39.9 m for S3 in RCP 8.5 by 2091. On average, the projected decrease in groundwater level is higher for the RCP 8.5 scenario than RCP 4.5.

The rate of decrease in groundwater level throughout the valley is not uniform. The decline in groundwater level in the centre of the valley is significant and much higher than the northern and southern areas. The result reveals that well H17 (Hotel Soaltee), in the central part of the valley, will experience the maximum decrease in groundwater level. The ACCESS-CSIRO-CCAM projects a maximum decrease of 133.5 m in well H17 (Hotel Soaltee) for RCP 8.5 scenario and 128.5 m for RCP 4.5 by 2091 under pumping scenario S3. Fig. 8 shows the decrease in groundwater level with respect to the observed groundwater level (2001) for three different time periods: 2031, 2061 and 2091 with S1, S2 and S3 for ACCESS-CSIRO-CCAM RCM and RCP scenarios 4.5 and 8.5. The decrease in groundwater level for CNRM-CM5-CSIRO-CCAM and MPI-ESM-LR-CSIRO-CCAM RCMs is presented in Supplementary Figs. S1 and S2.

These spatial differences in groundwater level might be linked to the level of groundwater abstraction by the density of the pumping wells. The central part of the valley is more densely populated with the greatest number of abstraction wells and withdraws the maximum amount of water for domestic, industrial and other economic activities. In contrast, the central part of Kathmandu Valley is a highly built-up area, reducing groundwater recharge to the aquifers.

4.6. Spatial variation in groundwater resiliency

The groundwater resiliency map of the Kathmandu Valley was developed based on the indicators described in Section 3.5.1 for all three pumping scenarios (S1, S2, S3) and three time periods (2031, 2061 and 2091) using three RCMs under both RCP scenarios (RCP 4.5 and RCP 8.5). The results show a projected decrease in the percentage of area under “very highly resilient” class and a projected increase in the “not resilient” class, towards the future periods. The decrease in the area classified as very highly resilient and an increase in the area under not resilient was significant and higher for pumping scenario S3 than S2 and S1. The maximum fluctuation in the percentage of area under five resiliency classes is shown by ACCESS-CSIRO-CCAM RCM. According to ACCESS-CSIRO-CCAM RCM for both RCP scenarios and pumping scenario S3, only 10.7% of the total area will be classified as very highly resilient by 2091. Under RCP 4.5 scenario and pumping scenario S3, 25.9% of the total area will be classified as not resilient by 2091. Likewise, for RCP 8.5 scenario and pumping scenario S3, 43.8% of the total area will be classified as not resilient class by 2091.

The result reveals that the majority of the area in central Kathmandu Valley is projected to fall under the “not resilient” and “fairly resilient” classes whereas the area in the southern and northern parts of the valley will be classified as “very highly” resilient and “highly resilient” for all three RCMs, pumping scenarios and RCP scenarios. Fig. 9 shows the groundwater resiliency map of Kathmandu Valley for three different time periods: 2031, 2061 and 2091 with S1,

S2 and S3 for ACCESS-CSIRO-CCAM RCM and RCP 4.5 and RCP 8.5 scenarios. Furthermore, the groundwater resiliency map of the Kathmandu Valley for CNRM-CM5-CSIRO-CCAM and MPI-ESM-LR-CSIRO-CCAM RCMs is presented in Supplementary Figs. S3 and S4.

5. Conclusions

The groundwater resiliency map of the Kathmandu Valley in Nepal was developed using the results from the hydrological model, groundwater model and three RCMs under RCP scenarios (RCP 4.5 and RCP 8.5). The results showed a projected increase in the future temperature (T_{max}, T_{min}) of the basin. By the end of the twenty-first century, the average annual maximum temperature is projected to increase by 0.4–2.2 °C in RCP 4.5 and 0.5–3.8 °C in the RCP 8.5 scenario. Likewise, the average annual minimum temperature is projected to increase by 0.5–2.4 °C in RCP 4.5 and 0.6–4.4 °C in RCP 8.5 scenario. As for precipitation, this is expected to decrease to the maximum level in the monsoon season (June–September) compared to the baseline period for all time horizons and both climate change scenarios. The decrease in precipitation ranges from 8.9 to 123 mm under RCP 4.5 and from 10.5 to 114.28 mm under the RCP 8.5 scenario.

The impact of climate change on groundwater recharge and groundwater level was also analysed. Future groundwater recharge is projected to decrease with the maximum decrease being in the monsoon season. The decrease in groundwater recharge ranges from 3.3 to 50.7 mm in the RCP 4.5 scenario and from 19 to 102.1 mm in RCP 8.5. The average groundwater level is projected to decrease in all three pumping scenarios (S1, S2 and S3) with a higher decrease for S3 than S2 and S1. The maximum decrease in average groundwater level ranges from 9.6 to 37.4 m for the RCP 4.5 scenario and 12–39.9 m for RCP 8.5. However, the decrease in groundwater level is uneven across the valley. The central part of the valley faces a higher decrease in groundwater level than the northern and southern areas. The area classified as “very highly resilient” is projected to decrease and that falling under the “not resilient” class is projected to increase in future under all pumping scenarios. Such decrease is projected to be more significant for S3 than scenario S2 and S1. The majority of the city area (centre) in the valley is projected to be “not resilient” and the northern and southern parts of the valley are likely to be “resilient” in all pumping scenarios.

Based on the results and variability in terms of climate change, it can be concluded that the groundwater resources in the valley are at risks due to climate change. Therefore, proper monitoring of the groundwater condition and development of adaptation is crucial for sustainable management of groundwater resources in the Kathmandu Valley.

Acknowledgements

This study was conducted under the project “Mapping groundwater resilience to climate change and human development in Asian cities” (CRRP 2018-01MY-Shrestha) supported by the Asia-Pacific Network on Global Change Research (APN). The authors would like to express sincere thanks to the Department of Hydrology and Meteorology (DHM) and Kathmandu Valley Water Supply Management Board (KVWSMB) for providing the required data for this research.

Appendix A. Supplementary data

Supplementary data to this article can be found online at https://doi.org/10.1016/j.envres.2020.109149.

References

Alansi, A.W., Amin, M.M., Abdul Halim, G., Shafri, H.Z.M., Aimrun, W., 2009. Validation of SWAT model for stream flow simulation and forecasting in Upper Bernam humid tropical river basin, Malaysia. Hydrol. Earth Syst. Sci. Discuss., 2009 7581–7609. https://doi.org/10.5194/hessd-6-7581-2009.

Ali, R., McFarlane, D., Verma, S., Dawes, W., Emelyanova, I., Hodgson, G., Charles, S., 2012. Potential climate change impact on groundwater resources of South-Western Australia. J. Hydrol. 475, 456–472.

Arias, M.E., Piman, T., Lauri, H., Cochrane, T.A., Kummu, M., 2014. Dams on Mekong tributaries as significant contributors of hydrological alterations to the Tonle Sap floodplain in Cambodia. Hydrol. Earth Syst. Sci. 18, 5303–5315.

Bates, B., Kundzewicz, Z., Wu, S., Palutikof, J., 2008. Climate Change and Water. IPCC, Geneva.

Cheng, T., Mo, Z., Shao, J., 2013. Accelerating groundwater flow simulation in MODFLOW using JASMIN-based parallel computing. Gr. Water 52 (2), 194–205. https://doi.org/10.1111/gwat.12047.

Cibin, R., Sudheer, K.P., Chaubey, I., 2010. Sensitivity and identifiability of stream flow generation parameters of the SWAT model. Hydrol. Process. 24 (9), 11331148. https://doi.org/10.1002/hyp.7568.

Cresswell, R.G., Bauld, J., Jacobson, G., Khadka, M.S., Jha, M.G., Shrestha, M.P., Regmi, S.R., 2001. A first estimate of ground water ages for the deep aquifer of the Kathmandu Basin, Nepal, using the radioisotope chlorine-36. Groundwater 39 (3), 321–474.

Emmanuel, O., 2008. Estimation of Groundwater Recharge in the Context of Future Climate Change in the White Volta River Basin, West Africa Doctoral Dissertation. Rheinischen Friedrich Wilhelms University.

Erturk, A., Ekdal, A., Gurel, M., Karakaya, N., Guzel, C., Gonenc, E., 2014. Evaluating the impact of climate change on groundwater resources in a small Mediterranean watershed. Sci. Total Environ. 499, 437–447.

Foster, S., MacDonald, A.M., 2014. The “water security” dialogue: why it needs to be better informed about groundwater. Hydrogeol. J. 22 (7), 1489–1492.

Gautam, D., Prajapati, R.N., 2014. Drawdown and dynamics of groundwater table in Kathmandu valley, Nepal. Open Hydrol. J. 8, 17–26.

Gunderson, L.H., 2000. Ecological resilience — in theory and application. Ecol., Evol. Syst. 31, 425–439.

IPCC, 2007. Climate Change 2007: Synthesis Report. Contribution of Working Groups I, II and III to the Fourth Assessment Report of the Intergovernmental Panel on Climate Change. Retrieved from, Geneva, Switzerland.

IS-1172:1993-Code of Basic Requirements for Water Supply, Drainage and Sanitation (Fourth Revision). Water Supply and Sanitation Sectional Committee, New Delhi, India.

Jha, M.G., Khadka, M.S., Shrestha, M.P., Regmi, S., Bauld, J., Jacobson, G., 1997. The Assessment of Groundwater Pollution in the Kathmandu Valley, Nepal: Report on Joint Nepal-Australia Project 1995–96. Australian Geological Survey Organization, Canberra, pp. 1–64.

IPCC, 2013. Climate Change 2013: The Physical Science Basis. Contribution of Working Group I to the Fifth Assessment Report of the Intergovernmental Panel on Climate Change. Retrieved from Cambridge, United Kingdom and New York.

Jha, M.G., Khadka, M.S., Shrestha, M.P., Regmi, S., Bauld, J., Jacobson, G., 1997. The assessment of groundwater pollution in the Kathmandu Valley, Nepal: report on Joint Nepal-Australia Project 1995–96. Australian Geological Survey Organization, Canberra, pp. 1–64.

Kemper, K., 2004. Groundwater from development to management. Hydrogeology. J. 12, 3–5 2004.

Kharin, V.V., Zwiers, F.W., Zhang, X., Wehner, M., 2013. Changes in temperature and precipitation extremes in CMIP5 ensemble. Clim. Change 111, 345–357. https://doi.org/10.1007/s10584-013-0705-8.

Koundouri, P., Groom, B., 2010. Groundwater management: an overview of hydrogeology, economic values and principles of management. Groundwater-Vol. III. Encyclopedia of Life Support Systems (EOLSS).

KUKL (Kathmandu Upatyaka Khanepani Limited), 2011. Kathmandu Upatyaka Khanepani Limited at a Glance. KUKL, Kathmandu Third Anniversary Report.

Lachaal, F., et al., 2012. Seismic, gravity, and wire line logging characterization of the Zéramdine fault corridor and its influence in the deep Miocene aquifers distribution (east-central Tunisia). Arabian J. Geosci. 8. https://doi.org/10.1007/s12517-011-0298-3.

Luo, Y., Zhang, X., Liu, X., Ficklin, D., Zhang, M., 2008. Dynamic modeling of organophosphate pesticide load in surface water in the northern San Joaquin Valley watershed of California. Environ. Pollut. 156, 1171–1181.

Maheswaran, G., Selvarani, A.G., Elanogvan, K., 2016. Groundwater resource exploration in Salem district, Tamil Nadu using GIS and remote sensing. J. Earth Syst. Sci. 125 (2), 311–328.

Moriasi, D.N., Arnold, J.G., Van Liew, M.W., Bingner, R.L., Harmel, R.D., Veith, T.L., 2007. Model evaluation guidelines for systematic quantification of accuracy in watershed simulations. Trans. ASABE 50 (3), 885. https://doi.org/10.13031/2013.23153.

Moss, R.H., Edmonds, J.A., Hibbard, K.A., Manning, M.R., Rose, S.K., Van Vuuren, D.P., 2010. The next generation of scenarios for climate change research and assessment. Nature 463 (7282), 747–756.

NGWA (National Groundwater Association), 2016. NGWA Consensus Definitions of Groundwater Sustainability and Resilience. [Available online, visited on 01 July 2018]. http://www.ngwa.org/Fundamentals/Pages/definitions.aspx.

Pandey, V.P., Chapagain, S.K., Kazama, F., 2010. Evaluation of groundwater environment of Kathmandu valley. Environ. Earth Sci. 60 (6), 1329–1342.

Pandey, V.P., Kazama, F., 2011. Hydrogeologic characteristics of groundwater aquifers in Kathmandu Valley, Nepal. Environ. Earth Sci. 62 (8), 1723–1732.

Pandey, V.P., Kazama, F., 2014. From an open-access to a state-controlled resource: the case of groundwater in the Kathmandu Valley, Nepal. Water Int. 39 (1), 97–112.

Pandey, V.P., Dhaubanjar, S., Bharati, L., Thapa, B.R., 2019. Hydrological response of Chamelia watershed in Mahakali basin to climate change. Sci. Total Environ. 650 (1),

365–383.
Pathak, D.R., Hiratsuka, A., Awata, I., Chen, L., 2009. Groundwater vulnerability assessment in shallow aquifer of Kathmandu valley using GIS-based DRASTIC model. Environ. Geol. 57 (7), 1569–1578.
Peters, E., van Lanen, H.A.J., Torfs, P.J.J.F., Bier, G., 2004. Drought in groundwater drought distribution and performance indicators. J. Hydrol. xx, 1–16.
Pholkern, K., Saraphirom, P., Srisuk, K., 2018. Potential impact of climate change on groundwater resources in the Central Huai Luang basin, North-East Thailand. Sci. Total Environ. 633, 1518–1535.
Piman, T., Lennaerts, T., Southalack, P., 2013. Assessment of hydrological changes in the lower Mekong basin from basin wide development scenarios. Hydrol. Process. 27, 2115–2125 doi: 10.1002/hyp.9764, 2013a.
Rogelj, J., Meinshausen, M., Knutti, R., 2012. Global warming under old and new scenarios using climate sensitivity range estimates. Nat. Clim. Chang. 2 (4), 248–253.
Santhi, C., Arnold, J., Williams, J., Dugas, W., Srinivasan, R., Hauck, L., 2001. Validation of the SWAT model on a large river basin with point and nonpoint sources. JAWRA J. Am. Water Resour. Assoc. 37 (5), 1169–1188 doi: 10.1111/j.1752-1688.2001.tb03630.x.
Sharma, U.C., Sharma, V., 2006. Groundwater sustainability indicators for the Brahmaputra basin in the north eastern region of India. In: Webb, B. (Ed.), Sustainability of Groundwater Resources and its Indicators. IAHS Publ. 302, IAHS Press, Foz do Iguacu, Brazil.
Shrestha, M., Acharya, S.C., Shrestha, P.K., 2017a. Bias correction of climate models for hydrological modelling – are simple methods still useful? Meteorol. Appl. 24 (3), 531–539. https://doi.org/10.1002/met.1655.
Shrestha, M.N., 2012. Groundwater use in Kathmandu Valley: an analysis of pre- and post Melamchi scenarios. In: Shrestha, S., Pradhananga, D., Pandey, V.P. (Eds.), Kathmandu Valley Groundwater Outlook, pp. 91–97 Kathmandu.
Shrestha, P.K., Shakya, N.M., Pandey, V.P., Birkinshaw, S.J., Shrestha, S., 2017b. Model-based estimation of land subsidence in Kathmandu Valley, Nepal. Geomatics, Nat. Hazards Risk 8 (2), 974–996. https://doi.org/10.1080/19475705.2017.1289985.
Shrestha, S., Bach, T.V., Pandey, V.P., 2016. Climate change impact on groundwater resources in Mekong Delta under representative concentration pathways (RCPs) scenario. Environ. Sci. Policy 61, 1–13.
Shrestha, S., Shrestha, M., Babel, M.S., 2017c. Assessment of climate change impact on water diversion strategies of Melamchi Water Supply Project in Nepal. Theor. Appl. Climatol. 128 (1), 311–323. https://doi.org/10.1007/s00704-015-1713-6.
Shrestha, S., Shrestha, M., Babel, M.S., 2017. Assessment of climate change impact on water diversion strategies of Melamchi Water Supply Project in Nepal. Theor. Appl. Climatol. 128, 311–323.
Teutschbein, C., Seibert, J., 2010. Regional climate models for hydrological impact studies at the catchment scale: a review of recent modelling strategies. Geography Compass 4 (7), 834–860. https://doi.org/10.1111/j.1749-8198.2010.00357.x.
Udmale, P., Ishidaira, H., Thapa, B.R., Shakya, N.M., 2016. The status of domestic water demand: supply deficit in Kathmandu valley, Nepal. Water 2016 8, 196. https://doi.org/10.3390/w8050196.
Uk Groundwater Forum, 2018. Groundwater Basics. [Available online, visited on 01 July 2018]. http://www.groundwateruk.org/Groundwater-Basics.aspx.
Vijaya, V.R.S., Sanjairaj, I., Goic, R., 2012. A review of climate change, mitigation and adaptation. Renew. Sustain. Energy Rev. 16 (1), 878–897 2012.
Vose, R.S., Easterling, D.R., Gleason, B., 2005. Maximum and minimum temperature trends for the globe: an update through 2004. Geophys. Res. Lett. 32, L23822. https://doi.org/10.1029/2005GL024379.
Yang, Y., Wang, G., Yu, J., 2010. Groundwater depth simulation based on Beijing country-level SWAT application tool. Water Sediment Sci. 309–317.
Yen, H., White, M.J., Jeong, J., Arabi, M., Arnold, J.G., 2015. Evaluation of alternative surface runoff accounting procedures using the SWAT model. Int. J. Agric. Biol. Eng. 8 (3), 64–68. https://doi.org/10.3965/j.ijabe.20150803.833.
Yoshida, M., Igarashi, Y., 1984. Neogene to quaternary lacustrine sediments in the Kathmandu valley, Nepal. J. Nepal Geol. Soc. 4, 73–100ip.
Zektser, L.S., Loaiciga, H.A., 1993. Groundwater fluxes in global hydrologic cycle: past, present, and future. J. Hydrol. 144, 405–427 1993.
Zhou, Y., Li, W., 2011. A review of regional groundwater flow modelling. Geosci. Front. 2 (2), 205–214.